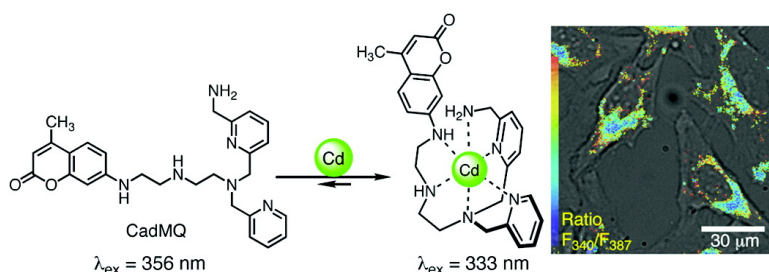


Fluorescence Imaging of Intracellular Cadmium Using a Dual-Excitation Ratiometric Chemosensor

Masayasu Taki, Mika Desaki, Akio Ojida, Shohei Iyoshi,
 Tasuku Hirayama, Itaru Hamachi, and Yukio Yamamoto

J. Am. Chem. Soc., **2008**, 130 (38), 12564-12565 • DOI: 10.1021/ja803429z • Publication Date (Web): 30 August 2008

Downloaded from <http://pubs.acs.org> on February 8, 2009



More About This Article

Additional resources and features associated with this article are available within the HTML version:

- Supporting Information
- Links to the 1 articles that cite this article, as of the time of this article download
- Access to high resolution figures
- Links to articles and content related to this article
- Copyright permission to reproduce figures and/or text from this article

[View the Full Text HTML](#)

Fluorescence Imaging of Intracellular Cadmium Using a Dual-Excitation Ratiometric Chemosensor

Masayasu Taki,^{*,†,‡} Mika Desaki,[†] Akio Ojida,[§] Shohei Iyoshi,[†] Tasuku Hirayama,[†] Itaru Hamachi,[§] and Yukio Yamamoto[†]

Graduate School of Human and Environmental Studies and Graduate School of Global Environmental Studies, Kyoto University, Yoshida, Sakyo-ku, Kyoto 606-8501, and Graduate School of Engineering, Kyoto University, Katsura Campus, Nishikyo-ku, Kyoto 615-8510, Japan

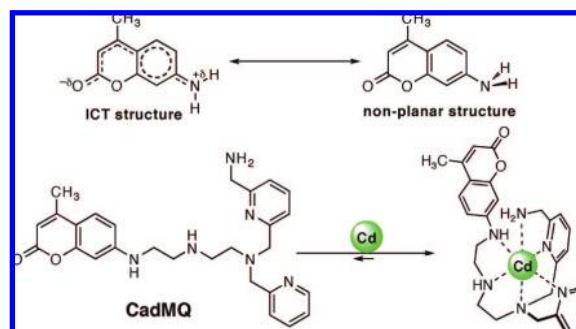
Received May 8, 2008; E-mail: taki@chem.mbox.media.kyoto-u.ac.jp

Cadmium (Cd), an inessential element for life, has been recognized as a highly toxic heavy metal and is listed by the U.S. Environmental Protection Agency as one of 126 priority pollutants. Humans are exposed to Cd²⁺ through the ingestion of contaminated food or water and inhalation of cigarette smoke. Cd²⁺ causes a number of lesions in many organs and tissues such as the kidney, liver, gastrointestinal tract, brain, and bone.¹ In addition, chronic exposure to Cd²⁺ has been implicated as a cause of cancers of the lung, prostate, pancreas, and kidney;² therefore, the International Agency for Research on Cancer (IARC) has classified cadmium and cadmium compounds as category I carcinogens.³ Although many experimental results have been obtained on the ability of Cd²⁺ to adversely affect cellular functions, the molecular mechanisms of Cd²⁺-uptake by cells as well as of carcinogenesis due to Cd²⁺ in humans and other mammals remains unclear.¹

Fluorescent sensors that can aid in the visualization of specific metal ions in living cells have been indispensable tools for understanding of biological phenomena.^{4,5} Many synthetic sensors that exhibit a fluorescence response to Cd²⁺ have been demonstrated; however, most of these sensors can respond to Zn²⁺ as well because the two metal cations often exhibit similar coordination properties.⁶ Hence, it has been a significant challenge to develop a Cd²⁺-selective fluorescent sensor that can discriminate Cd²⁺ from Zn²⁺ under physiological conditions.⁷ Recently, the research groups of Peng and of Wang have reported confocal images of Cd²⁺ in living cells using BODIPY- and fluorescein-based sensors, respectively; however, they have not shown the reversible binding of Cd²⁺ in these cells.^{7a,b} Furthermore, sensor molecules with higher affinity for Cd²⁺ than either BODIPY- or fluorescein-based sensors are required because cell growth and DNA synthesis would be significantly stimulated by Cd²⁺ concentrations as low as 100 pM,⁸ a level that lies beyond the detection limits of either of these sensors. Herein, we report a new Cd²⁺-selective fluorescent sensor, CadMQ. The excitation wavelength of this molecule exhibits a significant blue shift under physiological conditions when bound to Cd²⁺, thereby enabling dual-excitation ratiometric imaging of Cd²⁺, which can, in principle, provide accurate and quantitative measurements of metal ion concentrations in cells.

CadMQ consists of coumarin-120 (C120: 7-amino-4-methyl-1,2-benzopyrone), and a derivative of *N,N,N',N'*-tetrakis(2-pyridylmethyl)ethylenediamine (TPEN) as the chelator. It has been proposed that C120 exists in an intramolecular charge transfer (ICT) structure in higher polarity solvents, where the bond between the 7-amino group and the 1,2-benzopyrone moiety attains a substantial double bond character.⁹ In a nonpolar solvent, however, NH₂ nitrogen is

Scheme 1



bound to the benzopyrone moiety by a single bond, and the absorption energy has a higher value than it does in a polar solvent.⁹ We speculate that if the chelator, which can allow metal-ion binding with the 7-amino group on the coumarin ring, is incorporated into C120, the ICT structure may change into a nonplanar structure and therefore a blue shift of the excitation spectrum will be observed.¹⁰

Spectroscopic measurements of CadMQ were performed under physiological conditions (50 mM HEPES, pH 7.20, 0.1 M KNO₃). CadMQ exhibits an intense absorption band at 356 nm ($\epsilon = 1.77 \times 10^5 \text{ M}^{-1} \text{ cm}^{-1}$), suggesting the formation of the ICT structure in the excited state. Upon addition of Cd²⁺, a decrease in the absorbance of this band and a concomitant increase in that of a new band at 333 nm ($\epsilon = 1.42 \times 10^5 \text{ M}^{-1} \text{ cm}^{-1}$) were observed with a distinct isosbestic point at 340 nm. A significant hypsochromic shift of 23 nm of the absorption wavelength indicates coordination of the 7-amino group to Cd²⁺ to form the nonplanar structure (Scheme 1). The absorption bands at 356 and 333 nm linearly decreased and increased, respectively, up to a 1:1 [Cd²⁺]/[CadMQ] ratio, which is consistent with a 1:1 complex stoichiometry. The binding of Cd²⁺ resulted in a bathochromic shift of the emission maximum of only 4 nm; this wavelength shift is much less than that observed in the absorption titration. The quantum yields of the free ligand and Cd²⁺-bound forms were determined to be 0.59 and 0.70, respectively. Therefore, it can be concluded that CadMQ enables the calculation of [Cd²⁺]_{free} using the ratio of the fluorescence intensities at the different two wavelengths in the excitation spectrum. Figure 1a shows a set of excitation spectra for CadMQ in calibration buffers with various [Cd²⁺]_{free}. The apparent dissociation constant *K_d* for Cd²⁺ was determined to be 0.16 nM at pH 7.20 by plotting the fluorescence intensities at 328 or 368 nm against log[Cd²⁺]_{free} (Figure 1b). This nonlinear fitting analysis reveals that CadMQ is suitable to determine [Cd²⁺]_{free} between 40 and 660 pM. The fluorescence intensity of CadMQ changed with pH and reached a maximum at pH 6.3 (Supporting Information, Figure S2). However, a significant shift of the fluorescence wavelength was not observed; accordingly, the

[†] Graduate School of Human and Environmental Studies.

[‡] Graduate School of Global Environmental Studies.

[§] Graduate School of Engineering.

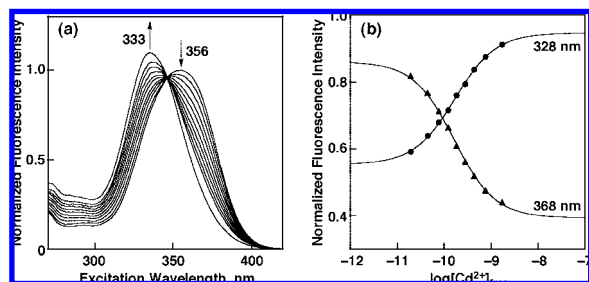


Figure 1. (a) Excitation spectra of CadMQ ($2.5 \mu\text{M}$) monitored at 440 nm in $\text{Cd}^{2+}/\text{Mg}^{2+}/\text{EDTA}$ buffered system (50 mM HEPES, pH 7.20, 0.1 M KNO_3 ; 1 mM EDTA, 10 mM MgSO_4 , 0–0.9 mM CdCl_2) and in 50 mM HEPES buffer (pH 7.20) containing $\sim 20 \mu\text{M}$ CdCl_2 . (b) Plots of fluorescence intensities at 328 (circle) and 368 (triangle) nm with best-fit curves for the dissociation constant 1.62×10^{-10} M.

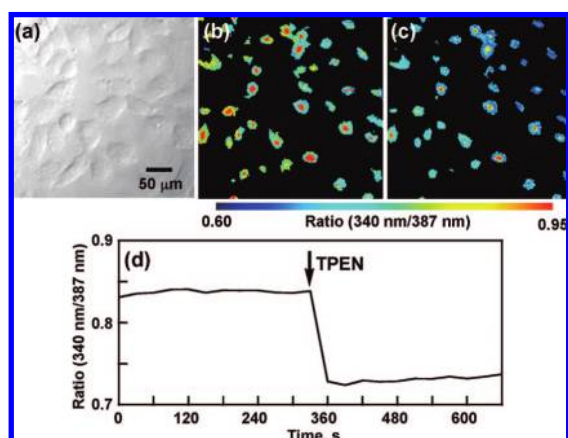


Figure 2. Ratio images of Cd^{2+} in HeLa cells exposed to $5 \mu\text{M}$ of Cd^{2+} for 3 h at 37°C , then further incubated with $5 \mu\text{M}$ CadMQ for 10 min at 37°C . Images were taken every 30 s: (a) bright-field transmission image; (b) ratio image (340 nm/387 nm) of CadMQ-stained cells prior to TPEN treatment; (c) ratio image of the same cells after treatment with $200 \mu\text{M}$ TPEN. The image is of the system at 360 s. (d) Average ratio of cells (340 nm/387 nm, $N > 10$) at the corresponding time.

fluorescence ratios between 333 and 356 nm changed only slightly over the wide range of pH.

A large hypsochromic shift in the excitation spectrum observed with Cd^{2+} is unaffected by the presence of high concentrations of Na^+ , K^+ , Mg^{2+} , and Ca^{2+} (>5 mM), indicating that this probe will be useful in a wide range of biological and microscopic applications. Some of the transition metal ions including Cu^{2+} , Zn^{2+} , and Hg^{2+} interfered with Cd^{2+} binding (Figure S4), which suggests competing binding of these cations.¹¹ It should be noted that the addition of Zn^{2+} resulted in a slight hypsochromic shift of CadMQ in the excitation spectrum, and little affected the fluorescence ratio. Such the difference in the fluorescence response of CadMQ toward Zn^{2+} and Cd^{2+} can be supported by ^1H NMR spectra in D_2O (pD 7.6, Figure S6). Complexation with Cd^{2+} induced downfield shifts of the coumarin moiety whereas slight upfield shifts were observed for Zn^{2+} complex. This observation strongly demonstrates that the 7-amino group of the coumarin interacts with Cd^{2+} , but not with Zn^{2+} .

Incubation of HeLa cells with $5 \mu\text{M}$ CadMQ for 30 min at 37°C revealed a bright punctate staining pattern, indicating that this molecule is membrane permeable. To determine the intracellular distribution of CadMQ, cells were coincubated with LysoTracker Red. A complete overlap of the images between CadMQ and LysoTracker Red revealed that our sensor molecule was located within the acidic compartments

of the cells (Figure S7). Subsequent experiments of Cd^{2+} -imaging in living cells were performed with a ratio imaging system. Cells were exposed to $5 \mu\text{M}$ Cd^{2+} for 3 h at 37°C , washed with PBS containing $200 \mu\text{M}$ EDTA to remove extracellular Cd^{2+} , and further incubated with $5 \mu\text{M}$ CadMQ for 10 min. The fluorescence ratio between the intensities of the 340 and 387 nm bands remained unchanged for 330 s; however, this immediately changed (within 30 s) upon the addition of the heavy metal chelator TPEN ($200 \mu\text{M}$) to the medium (Figure 2). A decrease and increase in the fluorescence intensities at 340 and 387 nm, respectively, induced by TPEN treatment indicate that CadMQ can probe the change in the intracellular Cd^{2+} levels (Figure S9). In the control experiment, by contrast, initial fluorescence intensity ratio for cells grown without Cd^{2+} was lower than that for Cd^{2+} -exposed cells (Figure S10). In fact, a negligible change in the ratio was observed upon the addition of TPEN.

In conclusion, we have developed a ratiometric fluorescent sensor for Cd^{2+} , CadMQ. This probe exhibits excellent Cd^{2+} -selectivity over other transition metal ions in aqueous media, including Zn^{2+} . It also has high quantum yields in both the apo and Cd^{2+} -bound forms, a strong affinity for Cd^{2+} , and membrane permeability. The ratio-imaging experiments demonstrate that CadMQ will be a useful tool for detecting changes in Cd^{2+} concentrations in living mammalian cells.

Acknowledgment. We thank Professor Y. Mori and Dr. S. Kiyonaka at Kyoto University for helpful advice. This work was financially supported by Grant-in-Aid for Young Scientists (B) (No. 17750155 to M.T.) from JSPS.

Supporting Information Available: Synthesis and characterization of CadMQ, UV–vis titration for Cd^{2+} , pH-titration, confocal images, and experimental details. This material is available free of charge via the Internet at <http://pubs.acs.org>.

References

- (1) (a) Waisberg, M.; Joseph, P.; Hale, B.; Beyersmann, D. *Toxicology* **2003**, *192*, 95–117. (b) Zalups, R. K.; Ahmad, S. *Toxicol. Appl. Pharmacol.* **2003**, *186*, 163–188. (c) Bridges, C. C.; Zalups, R. K. *Toxicol. Appl. Pharmacol.* **2005**, *204*, 274–308.
- (2) (a) Waalkes, M. P. *J. Inorg. Biochem.* **2000**, *79*, 241–244. (b) Waalkes, M. P.; Coogan, T. P.; Barter, R. A. *Crit. Rev. Toxicol.* **1992**, *22*, 175–201.
- (3) *Monographs on the Evaluation of the Carcinogenic Risk of Chemicals to Humans*; Beryllium, Cadmium, Mercury, and Exposures in the Glass Manufacturing Industry, Vol. 58; International Agency for Research on Cancer: Lyon, France, 1993.
- (4) (a) de Silva, A. P.; Gunaratne, H. Q. N.; Gunlaugsson, T.; Huxley, A. J. M.; McCoy, C. P.; Rademacher, J. T.; Rice, T. E. *Chem. Rev.* **1997**, *97*, 1515–1566. (b) Valeur, B. *Molecular Fluorescence: Principles and Applications*; Wiley-VCH: Weinheim, NY, 2002. (c) Domaille, D. W.; Que, E. L.; Chang, C. J. *Nat. Chem. Biol.* **2008**, *3*, 168–175.
- (5) Hinkle, P. M.; Shanshala, E. D.; Nelson, E. J. *J. Biol. Chem.* **1992**, *267*, 25553–25559.
- (6) (a) Nolan, E. M.; Ryu, J. W.; Jaworski, J.; Feazell, R. P.; Sheng, M.; Lippard, S. J. *J. Am. Chem. Soc.* **2006**, *128*, 15517–15528. (b) Goldsmith, C. R.; Lippard, S. J. *Inorg. Chem.* **2006**, *45*, 555–561. (c) Komatsu, K.; Kikuchi, K.; Kojima, H.; Urano, Y.; Nagano, T. *J. Am. Chem. Soc.* **2005**, *127*, 10197–10204. (d) Aoki, S.; Kagata, D.; Shiro, M.; Takeda, K.; Kimura, E. *J. Am. Chem. Soc.* **2004**, *126*, 13377–13390. (e) Maruyama, S.; Kikuchi, K.; Hirano, T.; Urano, Y.; Nagano, T. *J. Am. Chem. Soc.* **2002**, *124*, 10650–10651. (f) Taki, M.; Wolford, J. L.; O'Halloran, T. V. *J. Am. Chem. Soc.* **2004**, *126*, 712–713. (g) Henary, M. M.; Wu, Y. G.; Fahrni, C. J. *Chem.–Eur. J.* **2004**, *10*, 3015–3025.
- (7) (a) Peng, X. J.; Du, J. J.; Fan, J. L.; Wang, J. Y.; Wu, Y. K.; Zhao, J. Z.; Sun, S. G.; Xu, T. *J. Am. Chem. Soc.* **2007**, *129*, 1500–1501. (b) Liu, W. M.; Xu, L. W.; Sheng, R. L.; Wang, P. F.; Li, H. P.; Wu, S. K. *Org. Lett.* **2007**, *9*, 3829–3832. (c) Choi, M.; Kim, M.; Lee, K. D.; Han, K. N.; Yoon, I. A.; Chung, H. J.; Yoon, J. *Org. Lett.* **2001**, *3*, 3455–3457. (d) Gunlaugsson, T.; Lee, T. C.; Parkesh, R. *Org. Lett.* **2003**, *5*, 4065–4068.
- (8) Vonzglimicki, T.; Edwall, C.; Ostlund, E.; Lind, B.; Nordberg, M.; Ringertz, N. R.; Wroblewski, J. *J. Cell Sci.* **1992**, *103*, 1073–1081.
- (9) Pal, H.; Nad, S.; Kumbhakar, M. *J. Chem. Phys.* **2008**, *119*, 443–452.
- (10) Mizukami, S.; Nagano, T.; Urano, Y.; Odani, A.; Kikuchi, K. *J. Am. Chem. Soc.* **2002**, *124*, 3920–3925.
- (11) K_d for Zn^{2+} was determined to be 44.6 pM. See Supporting Information.

JA803429Z